Effect of platinum group metal addition on microstructure and corrosion behaviour of Ti–47·5 at-%Al

I. A. Mwamba*[1,2], L. A. Cornish[2] and E. van der Lingen[3]

Plain and alloyed titanium aluminides of composition Ti–47·5 at-%Al were prepared with the addition of 1·0 at-% platinum group metals (PGMs). The as cast alloys were subjected to potentiodynamic scans in 5, 15 and 25 wt-%HCl solutions at room temperature, and the PGM containing alloys were assessed for their abilities to spontaneously passivate by cathodic modification. Plain titanium aluminide had a duplex microstructure consisting of lamellar (α_2 and γ alternating lamellae) and γ-TiAl phase grains. The introduction of 1·0 at-%PGMs (platinum, palladium and iridium) led to the formation of a new phase, developing more in the γ-TiAl phase grains and a general improvement of corrosion resistance by increasing the corrosion potential to nobler values. Platinum group metal additions to plain TiAl resulted in the corrosion potentials falling in the passive region of plain TiAl, indicating spontaneous passivation of PGM alloyed TiAl in 5 and 15 wt-%HCl solutions. In 25 wt-%HCl solution, the addition of PGMs shifted the cathodic process in the transpassive or active region of plain TiAl, resulting in either case in the dissolution of the alloy due to the absence of an extended passivation region. The cathodic modification of PGM alloyed TiAl occurred as a result of PGM accumulation on the surface of the TiAl alloys, which simultaneously improved the hydrogen evolution efficiency and inhibited anodic dissolution.

Keywords: Titanium aluminide, Cathodic modification, Passivation, Platinum group metals, Transpassive region, Active region, Passive region

Introduction

Titanium aluminides are alloys with high potential for elevated temperature applications in turbine components due to their strength at high temperatures, light weight and good oxidation properties.[1–5,] Much work has been dedicated to the investigation of the high temperature oxidation properties of titanium aluminides, resulting in various available data. Although significant research was carried out on the corrosion behaviour of pure titanium and titanium based alloys, very limited information is available on the room or near room temperature aqueous corrosion properties of titanium aluminides. The reason is that most investigations conducted on titanium aluminide alloys were aimed at high temperature performance, and therefore, high temperature properties such as oxidation and corrosion resistance were investigated. Gamma titanium aluminide, originally designed for high temperature applications, appears to have excellent potential for bone repair and replacement, with the biological response expected to be similar to other titanium based biomaterials.[6] These observations from early tests have triggered research activities on γ-TiAl for potential use as implants.[7] A growing interest in assessing the corrosion properties of γ-TiAl in aqueous media, simulating human body fluids, is taking place.[8]

In most aqueous environments, titanium and titanium alloys show good corrosion resistance due to the stable oxide films that form spontaneously on the surface. However, in chloride and/or fluoride solutions, titanium alloys are susceptible to attack, showing pitting and crevice corrosion.[9] Alloying elements, including nickel and molybdenum, have been added to titanium and titanium alloys to improve the corrosion resistance.[10] Precious metals were added to titanium to increase the corrosion resistance in non-oxidising acids.[11–14] Platinum group metal (PGM), nickel or molybdenum additions facilitate cathodic depolarisation by providing sites of low hydrogen overvoltage, which shifts the alloy potentials in the positive direction where oxide film passivation is possible. Relatively small concentrations of certain precious metals, in the order of 0·1 wt-%, are sufficient to significantly increase the corrosion resistance of titanium in reducing acid media. The addition of precious metals as

[1]Advanced Materials Division, Mintek, Randburg 2125, South Africa
[2]School of Chemical and Metallurgical Engineering and DST/NRF Centre of Excellence in Strong Materials, University of the Witwatersrand, Johannesburg 2001, South Africa
[3]Department of Engineering and Technology Management, Graduate School of Technology Management, University of Pretoria, Pretoria 0002, South Africa

*Corresponding author, email alainm@mintek.co.za

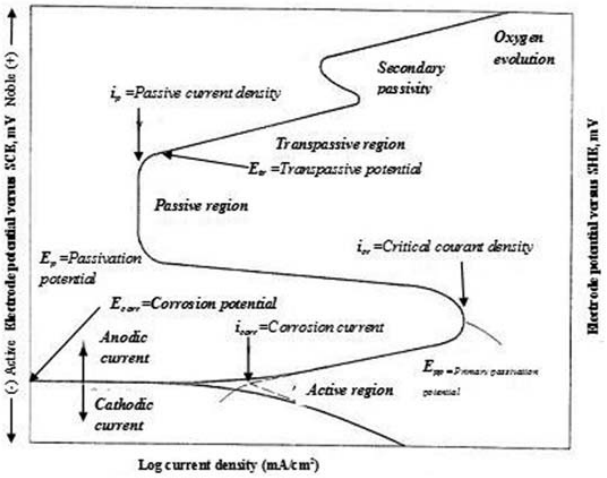

1 Typical polarisation scan of material exhibiting cathodic and anodic regions with active to passive transition[22]

alloying elements to improve the corrosion resistance is not limited to titanium and its alloys. Precious metals are also used to increase the corrosion resistance of stainless steels and nickel.[15–21] Figure 1 is a schematic diagram of a metal showing active to passive transition.

Their use for improving corrosion resistance originated in 1911 when Monnartz reported that the rapid corrosion of iron–chromium alloys in certain acids could be suppressed by winding a platinum wire around the corrosion test specimen or by adding platinum as an alloying element to steel.[18]

In this study, plain titanium aluminide of composition Ti–47·5 at-%Al and titanium aluminide with 1·0 at-%PGM additions were prepared and assessed for the effect of the PGMs on the microstructure and the cathodic modification during corrosion.

Experimental

Sample production

TiAl alloys were prepared by melting titanium grade 2 and aluminium of commercial purity in a button arc furnace under an argon atmosphere. The target composition was Ti–47·5 at-%Al. The melting cycle was repeated four times. Two types of alloys were prepared: plain TiAl and TiAl alloyed with 1·0 at-% PGMs (platinum, palladium, ruthenium and iridium). Different TiAl alloys were obtained containing PGMs substituting for titanium, with the aluminium content remaining at 47·5 at-%.

Microstructure characterisation

The samples were cut, polished and observed with optical and SEM microscopes. Scanning electron microscope imaging and EDX were conducted with a FEI Nova NanoSEM, a high resolution SEM. The chemistry of the samples and the phases were determined using a combination of X-ray diffraction and EDX. For X-ray diffraction, the samples were analysed with a PANalytical X'Pert Pro powder diffractometer with an X'Celerator detector and variable divergence and fixed receiving slits with Fe filtered Co K_α radiation. Phase identification was conducted using a X'Pert Highscore plus software.

Electrochemical tests

Potentiodynamic scans and open circuit potential (OCP) measurements were conducted with an ACM AutoTafel potentiostat/galvanostat system using a conventional three-electrode system with a saturated calomel electrode (SCE). For each alloy system, tests were performed in 5, 15 and 25 wt-%HCl at room temperature to assess the effect of the solution concentration on the corrosion rate. Scans were conducted with plain aluminides ($\alpha_2+\gamma$-TiAl) and aluminides with addition of precious metals.

A copper wire was soldered onto the sample, and the sample was cold mounted using a Struers Epofix resin and hardener and left for 12 h to cure. The wire soldered on the sample was placed inside the glass specimen holder, sealed with silicone and left for 3 h to cure. Each sample was ground to 1200 grit SiC paper finish, degreased with methanol, rinsed with distilled water and dried before being immersed in the solution. Polarisation diagrams were determined for the individual metals as well as for the galvanic couples using an ACM AutoTafel potentiostat/galvanostat system and a conventional three-electrode electrochemical cell fitted with a SCE as reference electrode and graphite as counter electrode. The surface was prepared just before starting the polarisation experiment to limit long term oxidation. Before conducting the scan, each sample was immersed in the solution for ~60 min to obtain a stable corrosion potential. Potentiodynamic scans were conducted by scanning from −350 to +1000 mV versus the corrosion potential at a scanning rate of 10 mV min^{-1}. The OPC tests were run for 15 h, during which the samples were exposed to a 5 wt-%HCl solution.

Results and discussion

Microstructural characterisation of alloys and hardness

The duplex microstructure in the plain TiAl alloy is shown in Fig. 2. Figure 2*a* shows that at a target composition of Ti–47·5 at-%Al, the microstructure was duplex, consisting of lamellar grains (area 1) with single phase regions between them (area 2). The grains identified in area 1 comprised alternating light and dark lamellae. In some parts, the lamellar grains were adjacent. Figure 2*b* shows, at higher magnification, such an area that appears to be only lamellar. This figure also shows that different grains could be identified by the orientation of their lamellae (areas 3–5).

Typical EDX results of plain TiAl are reported in Table 1. The overall composition in Table 2 indicates the formation of a duplex TiAl compound, according to the Ti–Al phase diagram shown in Fig. 2.[23] The Ti–Al phase diagram (Fig. 3) shows that Ti_3Al has an aluminium content between 22 and 33·5 at-% at 400°C. Between 33·5 at-% to composition of ~49·5 at-%Al at 400°C is the $Ti_3Al+\gamma$-TiAl two-phase field, which was these samples, with the lamellar region having a composition close to 47·5 at-%Al. The EDX results, together with the Ti–Al phase diagram, also show that area 1 in Fig. 2*a* comprised alternating Ti_3Al (α_2) and γ-TiAl. In the single phase regions (area 2 in Fig. 2*a*), the aluminium content was >50 at-%, showing the sole presence of γ-TiAl. These observations indicated that the microstructure was a mixture of lamellar grains (with alternating α_2 and γ parallel phases) and γ-TiAl grains between the lamellar grains, which is a typical duplex microstructure.[3,]

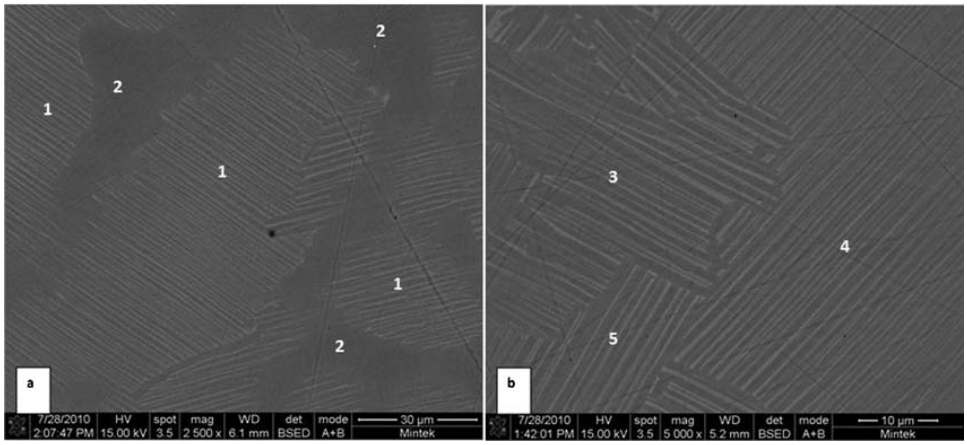

2 Image (SEM-BSE) of plain TiAl showing Ti_3Al (bright) and γ (dark) phases

Typical SEM and EDX results of TiAl alloys containing 1·0 at-%Ru are presented in Fig. 4 and Table 3 respectively. The SEM showed (Fig. 4) that the duplex structure was maintained in spite of the ruthenium addition. In addition, the precipitation of a light phase was observed mainly in the γ-phase regions. The shape of these precipitates was irregular, with no particular trend. This microstructure was also observed in samples doped with other PGMs.

The EDX results in Table 3 showed that the light phases had a higher Ru content than the lamellar and γ phases. The ruthenium content observed in the lamellar grain and γ-TiAl was <1 at-%, which is in the range reported by Khataee *et al.*[24] In a constitutional study of the Ti–Al–Ru system, they concluded that the solubility of ruthenium in γ is higher than in the α_2 (Ti_3Al) phase with reported values of ~0·5 at-%Ru in α_2 and less or equal to 1 at-% in γ-TiAl.

The Al–Ru–Ti isothermal section (Fig. 5) shows that the light phase reported in Table 3 (6·4–10·0 at-%Ru) is located in the phase field containing γ-TiAl and was named G-phase. The EDX results of the G-phase were affected by the surrounding matrix, so that the true value should be extrapolated away from the matrix phase(s). The G-phase is the $Al_{16}Ru_8Ti_6$ ternary compound with the $Mn_{23}Th_6$ structure, a D8a type crystal structure with a complex unit containing 116 atoms based on a body centred cubic structure.[24] The introduction of precious metal led to the precipitation and progression of the new phase in the γ grains, as shown in Fig. 5. In some areas, the growth of the G-phase in the γ grains resulted in a complete separation of lamellar grains.

Table 1 Energy dispersive X-ray spectroscopy analysis of plain TiAl (five analyses)

		Elemental composition/at-%	
Plain TiAl	Area	Ti	Al
	Overall	52·0±1·0	48·0±1·0
	Lamellae 1	52·7±0·7	47·3±0·7
	Plain 2	49·4±1·8	50·6±1·8

Table 2 Elemental composition of alloys

	PGM content/at-%					
Compound	Ti	Al	Ru	Pd	Pt	Ir
Plain TiAl	52·5	47·5	…	…	…	…
TiAl-1Ru	51·5	47·5	1	…	…	…
TiAl-1Pd	51·5	47·5	…	1	…	…
TiAl-1Pt	51·5	47·5	…	…	1	…
TiAl-1Ir	51·5	47·5	…	…	…	1

Effect of PGMs on corrosion behaviour

Electrochemical behaviour

A summary of the test results is given in Table 4, showing the current density, corresponding corrosion rate and corrosion potentials at each concentration of the HCl solution. The potentiodynamic scans of plain TiAl and TiAl–1Pd in solutions of different concentrations are shown below (Figs. 6 and 7).

Effect of alloying addition on corrosion potential

Corrosion of plain TiAl

In the 5 wt-%HCl solution, plain duplex titanium aluminide (Table 4 and Fig. 6) had a corrosion potential of about −605 V, which decreased as the concentration of the HCl solution increased. Thus, the primary active to passive zone decreased with increasing concentration of HCl solution. In all solution concentrations, pitting corrosion occurred as can be seen with the increase in current after passivation, e.g. transpassive region. Pitting corrosion occurred at potentials that decreased with increasing acid concentration. This observation is

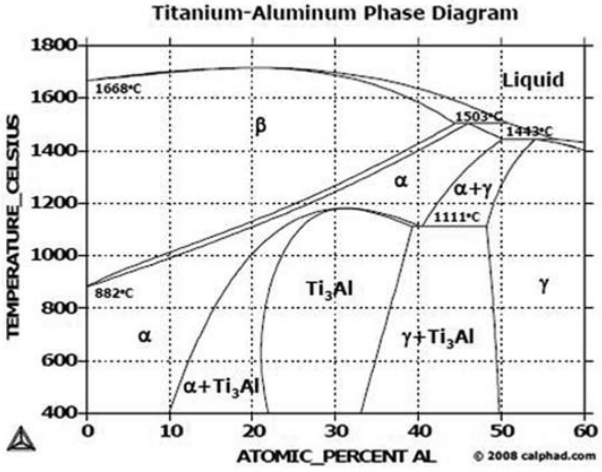

3 Ti–Al phase diagram[23]

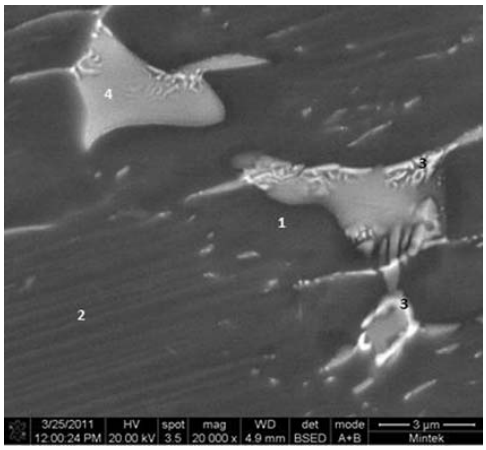

4 Images (SEM-BSE) of TiAl–0·2 at-%Ru alloy showing γ, α_2 and G-phase[3]

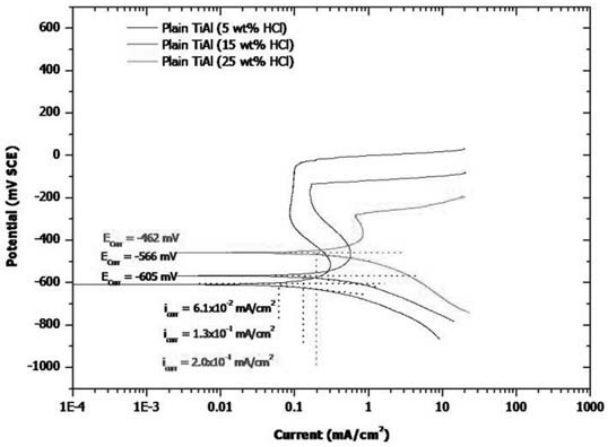

6 Potentiodynamic scans for plain TiAl ($\alpha_2+\gamma$) in HCl solution of different concentrations

in agreement with the work carried out by Saffarian *et al.*[25]

TiAl alloyed with PGMs

The addition of PGMs to duplex TiAl resulted in an increase in the corrosion potential (Table 4). Typical potentiodynamic scans are shown in Fig. 7 for duplex TiAl alloyed with 1·0 at-%Pd. The addition of palladium shifted the corrosion potential to nobler values. These results suggested that TiAl-1 at-%Pd will passivate spontaneously in 5, 15 and 25 wt-%HCl solutions. Similar results were obtained with TiAl–1·0 at-%Pt, TiAl–1·0 at-%Ru and TiAl–1·0 at-%Ir. Table 5 shows

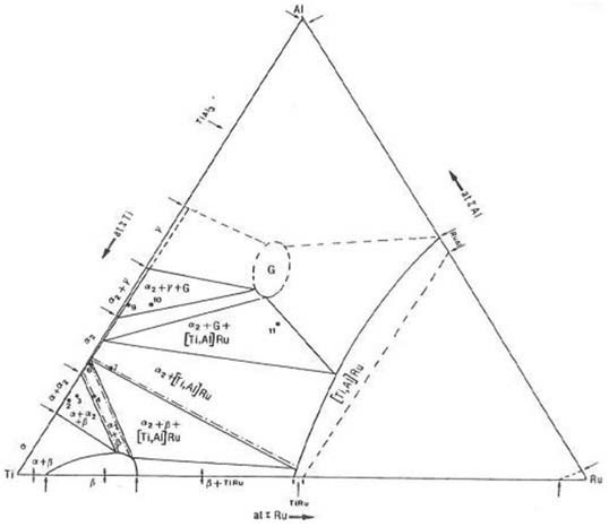

5 Isothermal section of ternary Ti–Al–Ru system at 770°C[24]

the potential increase observed with increasing solution concentration (5, 15 and 25 wt-%HCl) after 60 min exposure with reference to plain TiAl, as obtained by the following calculations

$$\Delta E_5 = E_5 - E_{\mathrm{TiAl}}$$

$$\Delta E_{15} = E_{15} - E_{\mathrm{TiA}}$$

$$\Delta E_{25} = E_{25} - E_{\mathrm{TiAl}}$$

where ΔE is the potential increase difference, E_5 is the corrosion potential in 5 wt-%HCl solution, E_{15} is the corrosion potential in 15 wt-%HCl solution, E_{25} is the corrosion potential in 25 wt-%HCl solution and E_{TiAl} is the corrosion potential of plain TiAl alloy.

The corrosion potential increases to nobler values are well illustrated (Fig. 8). The evolution of corrosion potentials with HCl concentration in the solution remains between −300 and −200 mV for TiAl containing PGMs, well above the evolution of the corrosion potential for plain TiAl, which remained below −450 mV. These graphs show clearly the shift of corrosion potentials to nobler values with the addition of PGMs to TiAl alloy and suggest an improvement in corrosion resistance.

Cathodic modification

The introduction of precious metals in plain TiAl resulted in a general improvement of corrosion resistance of the TiAl alloys by shifting the corrosion potentials to nobler values. However, the cathodic modification will be achieved only as follows:[26]

(i) when the plain duplex TiAl has a small critical current density i_{cr} that will be easily exceeded by the current of the hydrogen cathodic reaction on

Table 3 Typical EDX analysis of Ru containing TiAl (five analyses)

	Alloy TiAl–1Ru			
	Elemental composition/at-%			
Area	Ti	Al	Ru	Possible phase
Overall	49·3±0·3	49·3±0·3	1·0±0·1	γ,α_2, G-phase
Plain -1	46·9±1·5	52·4±1·7	0·7±0·1	γ-TiAl (Ru)
Striped -2	49·5±1·0	50·1±1·2	0·4±0·1	$\gamma+\alpha_2$ (Ru)
Light phase-3	42·0±0·2	48·2±1·9	9·8±2·6	G-phase
Grey-phase-4	53·2±0·8	40·5±0·7	6·3±0·3	G-phase

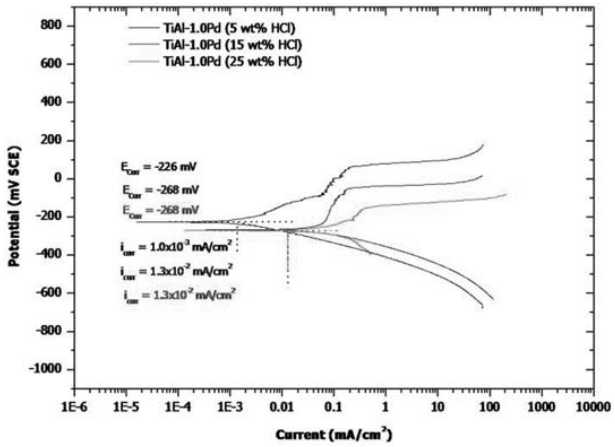

7 Potentiodynamic scans for TiAl+1·0 at-%Pd in HCl solution of different concentrations

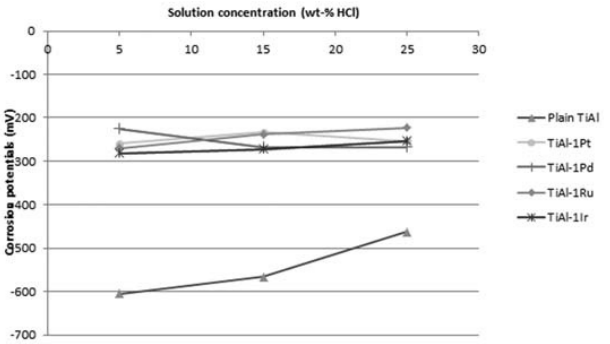

8 Variation of corrosion potential with solution concentration

TiAl with precious metal addition at the given passivation potential E_p. See schematic diagram in Fig. 1

(ii) if the passivation potential E_p of plain duplex TiAl is sufficiently negative to allow the cathodic component that has been introduced to change the corrosion potential E_{corr} of the TiAl with precious metal to a value in the passive range that is more positive than E_p but less positive than the potential associated with the onset of transpassive processes E_{tr}

(iii) when the transpassive potential E_{tr} of TiAl is sufficiently electropositive to allow a wide passivation region.

Table 6 shows the passivation regions obtained on the plain TiAl scans in the three solutions. This region decreased with increasing solution concentration and completely disappeared in 25 wt-%HCl solution. Whether the cathodic process of the TiAl alloyed with PGMs fell in the active, passive or transpassive region of the plain TiAl was verified by comparing the scans of PGM alloyed TiAl to the plain TiAl scans. Figure 9 shows the potentiodynamic scans of TiAl alloyed with PGMs superposed on the potentiodynamic scan of plain TiAl in 5 wt-%HCl. All the corrosion potentials of TiAl alloyed with PGMs fell in the passive region, suggesting that TiAl alloyed with PGMs would spontaneously passivate in the 5 wt-%HCl solution due to cathodic modification. A similar trend was observed in the 15 wt-%HCl solution, where all the cathodic processes of TiAl alloyed with PGMs fell within the passivation region (Fig. 10). It is worth saying that the same effect was achieved with 0·1–0·3 at-%Ru or Pd additions to titanium alloys in solutions of 1–5 wt-%HCl,[13] 0·2 at%Ru or Pd in 25 wt-%HCl.[11] However, in the 25 wt-%HCl solution, the corrosion potentials of TiAl alloyed with PGMs did not intersect the plain TiAl curve in the passive region (Fig. 11). While the cathodic process of TiAl alloyed with platinum and iridium

Table 4 Test parameters and resulting corrosion potentials, current densities and corrosion rates

Samples	HCl/wt-%	I_{corr}/mA cm^{-2}	Corr rate/mm/year	E_{corr}/mV(SCE)
Plain TiAl	5	0·061	0·549	−605
Plain TiAl	15	0·130	1·161	−566
Plain TiAl	25	0·200	1·764	−462
TiAl–1Pt	5	0·003	0·030	−260
TiAl–1Pt	15	0·011	0·099	−234
TiAl–1Pt	25	0·240	2·160	−254
TiAl–1Pd	5	0·001	0·009	−226
TiAl–1Pd	15	0·013	0·117	−268
TiAl–1Pd	25	0·013	0·117	−268
TiAl–1Ru	5	0·160	1·440	−270
TiAl–1Ru	15	0·930	8·370	−238
TiAl–1Ru	25	1·500	13·500	−223
TiAl–1Ir	5	0·026	0·234	−282
TiAl–1Ir	15	0·085	0·765	−272
TiAl–1Ir	25	0·096	0·864	−254

Table 5 Corrosion potential increases with precious metal addition

	Corrosion potentials/mV			Potential increase/mV		
Alloy	E_5	E_{15}	E_{25}	ΔE_5	ΔE_{15}	ΔE_{25}
Plain TiAl	−605	−556	−462	0	0	0
TiAl–1Pd	−226	−268	−268	379	288	194
TiAl–1Ru	−270	−238	−223	335	318	239
TiAl–1Pt	−260	−234	−254	345	322	208
TiAl–1Ir	−282	−272	−254	323	284	208

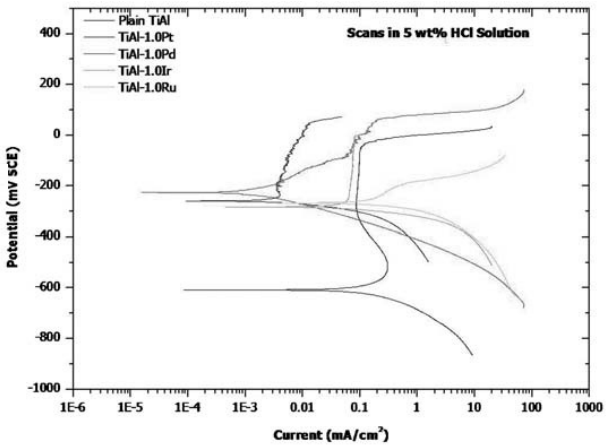

9 Effect of PGM additions on polarisation scans of TiAl in 5 wt-%HCl solution

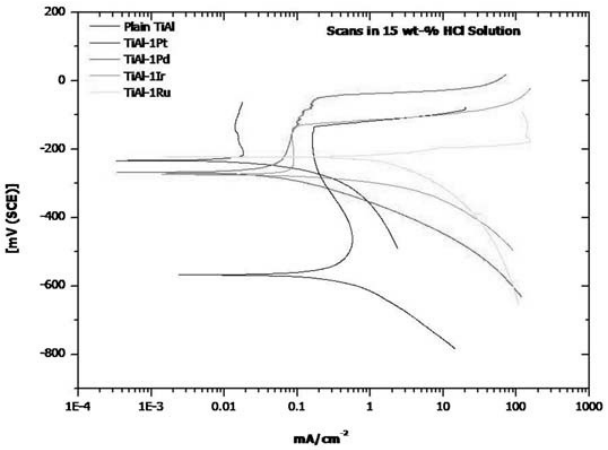

10 Effect of PGM additions on polarisation scans of TiAl in 15 wt-%HCl solution

intersected the plain TiAl curve in the transpassive region, the cathodic process of TiAl alloyed with palladium intersected the plain TiAl curve in the active region. In either case, this would result in alloy dissolution. This behaviour of the alloys in the 25 wt-%HCl solution suggested that it would be very difficult to improve the corrosion resistance of TiAl alloys by cathodic modification due to the fact that the passive region did not exist at all on the potentiodynamic scan of the plain TiAl immersed in 25 wt-%HCl solution (Table 6). These results showed that PGM alloyed TiAl would passivate spontaneously in 5 and 15 wt-%HCl solutions, whereas corrosion would take place in 25 wt-%HCl. This was due to the fact that a very large increase in corrosion potential (Table 3) resulted in the cathodic reaction of PGM alloyed TiAl intersecting the anodic reaction in the transpassive region of the plain TiAl, and an increase in current density occurred. This resulted in higher corrosion rates in PGM alloyed TiAl than Plain TiAl, although the corrosion potential values were nobler, as was the case for TiAl-1Ru, TiAl-1Pt and TiAl-Ir in 25 wt-%HCl solution. However, duplex stainless steel with 0·1 at-%Ru investigated both in low and high concentration solutions showed spontaneous passivation.[27,28]

Analysis of different parameters affecting corrosion behaviour

Solution concentration and corrosion rate

From Table 4, the corrosion rate histograms were drawn as functions of HCl concentration in solution and are presented in Fig. 12. These histograms show that in 5 and 15 wt-%HCl solutions, TiAl alloys with additions of palladium, platinum and iridium had low corrosion rates, indicative of good corrosion resistance. In 25 wt-%HCl solution, the corrosion rate of TiAl alloyed with platinum was higher than the corrosion rate of plain TiAl, even though the addition of platinum to

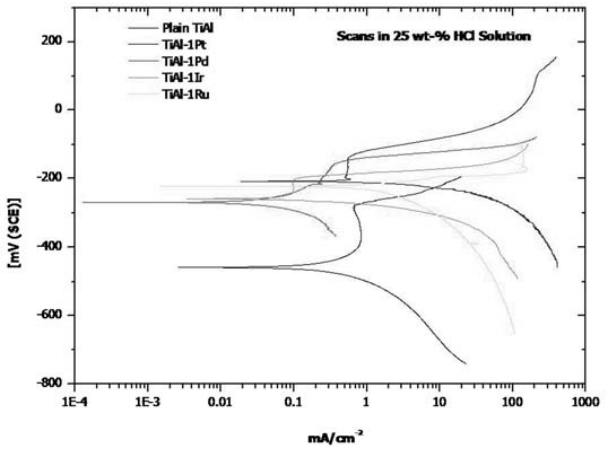

11 Effect of PGM additions on polarisation scans of TiAl in 25 wt-%HCl solution

TiAl, like other PGMs, shifted the corrosion potential to nobler values. This observation supported the fact that the high increase in corrosion potential of the Pt alloyed TiAl resulted in the cathodic process falling in the transpassive zone on the potentiodynamic scan of the plain TiAl (Fig. 11). Figure 12 also showed that the best performance in corrosion improvement was achieved with palladium addition. The addition of iridium resulted in a corrosion rate not significantly affected by the variation of HCl concentration in the solution. The corrosion rate of TiAl alloyed with ruthenium was higher than the corrosion rate of plain TiAl, even though the addition of ruthenium to TiAl, like other PGMs, shifted the corrosion potential to nobler values. This observation is strange as it does not support the fact that ruthenium also promoted cathodic modification. However, previous work has also shown that

Table 6 Characteristic values of potentials and current density for plain TiAl

Characteristic values of potential or current density	Solution concentration/wt-%HCl		
	5	15	25
E_{pa}/mV	−296	−251	−282
E_{pit}/mV	−48	−138	−281
Passivation region	From −296 to −48	From −251 to −138	∼0

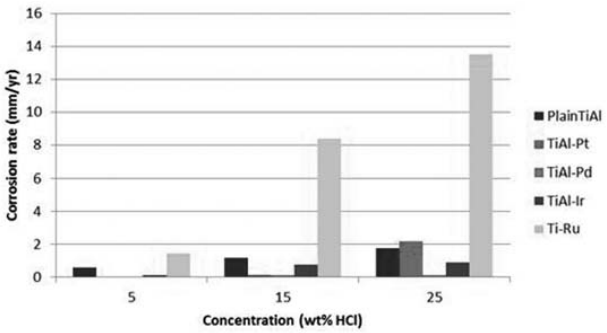

12 Corrosion rates of TiAl alloys with PGM additions in 5, 15 and 25 wt-%HCl solutions

ruthenium addition tended to shift the potentiodynamic scan towards high current density.[11]

Accumulation of precious metals on corroded TiAl alloys

The accumulation of precious metal on the surface of TiAl can be explained by the corrosion behaviour of PGMs, as presented by Pourbaix *et al.*[29] Platinum, palladium, ruthenium and iridium are very noble metals since, in the potential pH diagrams, their domains of stability cover most of the stability domain of water. According to their respective potential pH diagrams, they are thermodynamically stable in the presence of aqueous solutions of any pH with the exception of strong oxidising agents and complexing substances. At temperatures ~25°C, they remain unaltered in the presence of water or in aqueous solutions of caustic alkalis.

The best known reagent for dissolving platinum, aqua regia, acts by means of a combination of oxidising and complexing actions. Hydrochloric acid, which does not attack platinum on its own, will attack it when it contains chlorine in solution, because it then combines oxidising and complexing actions. Aqua regia (a mixture of hydrochloric and nitric acids) dissolves platinum slowly as chloroplatinic acid $PtCl_6H_2$ with the formation of the complex hexachloroplatinic(IV) acid $H_2[PtCl_6].6H_2O$.

Palladium is unattacked by water, except at high temperatures, and is not tarnished in moist air. Non-oxidising acids, acetic, hydrofluoric, oxalic and sulphuric acids are without action at ordinary temperatures.[29] Dilute nitric acid attacks palladium only slowly, but the metal is corroded quite rapidly by the concentrated acid. At 25°C, iridium is unattacked by water, solutions of caustic alkalis, acids and oxidising agents, including aqua regia. Ruthenium is less noble than the three other platinum metals. Although ruthenium is not attacked by water or non-complexing acids, it is easily corroded by oxidising alkaline solutions, such as peroxides and alkaline hypochlorites.

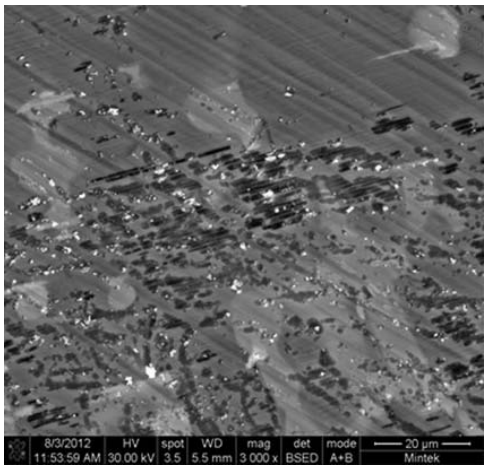

13 Image (SEM-BSE) of surface of TiAl–1·0 at-%Pt after potentiodynamic scan in 25 wt-%HCl solution

The solutions used in this work were 5 wt-%HCl (pH 0·11), 15 wt-%HCl (pH −0·52) and 25 wt-%HCl (pH −0·62). In these conditions, titanium and aluminium of the matrix and the precious metal rich phase were expected to be dissolved, leaving behind particles of high precious metal content on the surface (Fig. 13). The EDX results revealed that the precious metal content in these particles was very high (Table 7), suggesting that these particles were losing titanium and aluminium by dissolution. The poor corrosion resistance performance observed with titanium aluminide alloyed with ruthenium is in agreement with the conclusion made by Pourbaix *et al.*[29] that ruthenium was less noble than the other PGMs and more easily corroded. In terms of the cathodic modification process, even though the corrosion potential of Ti–47·5 at-%Al was shifted to the passive region by the addition of ruthenium, the exchange current density was very high, explaining the high corrosion rate observed in TiAl–1·0 at-%Ru.

The shift of corrosion potentials to nobler values was attributed to the accumulation of precious metals on the surface of TiAl alloys, which simultaneously improved the hydrogen evolution efficiency and inhibited anodic dissolution.[16] To confirm these explanations, SEM and EDX were conducted on the corroded surfaces to evaluate the precious metal content on the surfaces of alloys subjected to potentiodynamic scans in 25 wt-%HCl solution. The corrosion tests corresponded to an exposure of samples to 25 wt-%HCl solutions for 180 min, 30 min of which were in OCP. The EDX results are shown in Table 8, and the SEM images are

Table 7 Energy dispersive X-ray spectroscopy analysis of light particle phases on corroded surface of different alloys

	Precious metal content in light/high intensity particles of different alloys/at-%			
Elements	TiAl–1Pt	TiAl–1Pd	TiAl–1Ir	TiAl–1Ru
Al	44·7	45·3	50·4	43·3
Pt	13·7	…	…	…
Pd	…	8·8	…	…
Ir	…	…	4	…
Ru	…	…	…	13
Ti	41·6	45·9	45·6	43·7
Total	100	100	100	100

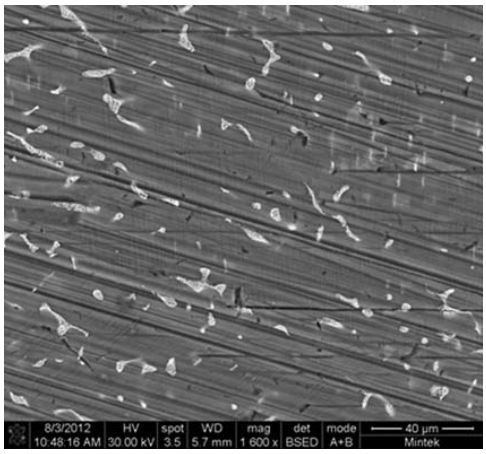

14 Image (SEM-BSE) of surface of TiAl–1·0 at-%Ir after potentiodynamic scan in 25 wt-%HCl solution

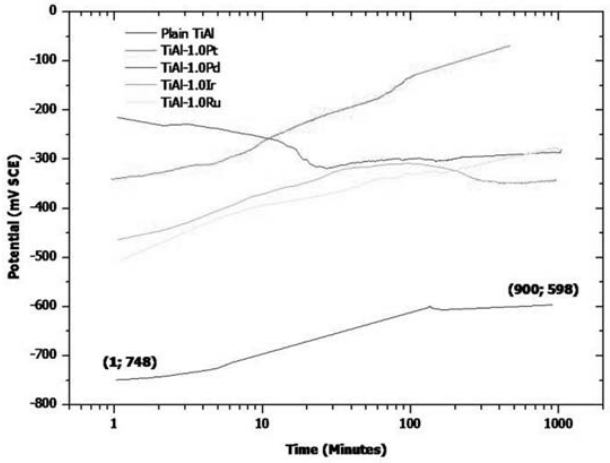

15 Open circuit potential curves for Ti–47·5 at-%Al alloyed with various PGMs tested in 5 wt-%HCl

shown in Figs. 13 and 14 for Pt alloyed TiAl and Pd alloyed TiAl respectively. Overall, there was an increase in PGM content on the surface of the different TiAl alloys, from 1·0 at-% in the as cast alloys to a maximum of 2·7 at-% for Ru alloyed TiAl. Typical bright phase particles of high PGM content are shown in Fig. 16 for Pt alloyed TiAl. Similar microstructures were observed when palladium and iridium were added to plain TiAl. The PGM content on the surfaces of the different alloys in Table 8 shows a clear increase, confirming that an accumulation in precious metal took place on the surfaces during the corrosion process. Iridium alloyed TiAl showed the lowest increase, which is in agreement with the moderate effect of the HCl concentration on its corrosion rate and the low amount of pits observed on the corroded samples (Fig. 14).

Open circuit potential measurements

The OPC tests were run for 15 h, during which the samples were exposed to a 5 wt-%HCl solution. The results of the tests are presented in Fig. 15 and Table 9, where the corrosion potential (mV) is reported as a function of time (min) in an open circuit. The general trend was a continuous increase in the corrosion potential with time to a value between −350 and −200 mV, suggesting that the samples became less active. Titanium aluminide alloyed with palladium showed a large decrease in corrosion potential in the first 30 min, indicative of an increase in activity, followed by a continuous increase up to the end of the test. The corrosion potential at the end of the test remained low at −286 mV after 15 h. Even though TiAl with palladium showed a potential decrease from 0 to ~30 min, the decrease remained higher than −350 mV, which was well above all the other corrosion potentials observed at 1 min. At that time, the corrosion potential was −500 mV for TiAl alloyed with ruthenium, −341 mV for TiAl alloyed with platinum and −466 mV for TiAl alloyed with iridium. Platinum alloyed TiAl showed a very high increase in corrosion potential and was above −100 mV after 15 h of exposure. This behaviour is in agreement with the high corrosion rate observed with this alloy during potentiodynamic scan in 25 wt-%HCl. An exposure to a relatively less aggressive solution for a long

Table 8 Energy dispersive X-ray spectroscopy analysis of alloy surface after potentiodynamic tests in 25 wt-%HCl solution

	Surface composition after corrosion test/at-%)					
Alloy	Al	Ti	Pd	Pt	Ir	Ru
TiAl–1Pd	52·6±1·7	45·0±1·4	2·4±0·3	…	…	…
TiAl–1Pt	49·9±0·1	48·9±0·1	…	1·2±0·1	…	…
TiAl–1Ir	50·1±0·5	48·8±0·4	…	…	1·2±0·1	…
TiAl–1Ru	39·3±3·6	58·0±3·1	…	…	…	2·7±0·6

Table 9 Starting and finishing OCPs

	Open circuit potential/mV(SCE)		Potential variation/mV(SCE)
Alloy	Potential start at 1 min	Potential end at 900 min	
Plain TiAl	−748	−598	150
TiAl–1Pt	−341	−70	271
TiAl–1Pd	−214	−286	−72
TiAl–1Ru	−510	−285	225
TiAl–1Ir	−466	−340	126

time would lead to the same results as an exposure to a more aggressive solution for a short period of time. Iridium and palladium alloyed TiAl showed small variation of OCP with time, indicating that the addition of iridium and palladium to TiAl resulted in an alloy that showed some stability towards the solution. This observation is consistent with the low variations in corrosion rate observed in these alloys (Fig. 12).

The shift of OCP towards nobler or less active potentials before stabilising is usually attributed to the progressive formation of a passive oxide film on the sample surface during immersion. Stabilisation at active potentials is due to the breakdown of the passive film as dissolution takes place. The tested samples did not exhibit potential stabilisation but rather a continuous increase in potential. The continuous increase in OCP was due to the accumulation of precious metal on the surface of the samples. As the amount of precious metal increased, the OCP shifted to nobler values. However, the displacement of OCPs to values in excess of the passivation potential of the plain Ti–Al alloy into its passive range was an indication that there was a secondary process of spontaneous passivation and oxide film formation, or at least partial oxide formation, also at play and contributing to the displacement of the corrosion potentials of the alloys containing PGMs to more noble values.

Conclusions

Titanium aluminide of composition Ti–47·5 at-%Al has a duplex microstructure consisting of lamellar (α_2 and γ alternating lamellae) and γ-TiAl phase grains. The introduction of 1·0 at-% PGMs (platinum, palladium and iridium) resulted in the formation of a new phase, developing more in the γ-TiAl phase grains and an improvement of the corrosion resistance by cathodic modification.

The cathodic modification was achieved in solutions of low acidic concentration. Platinum, palladium and iridium additions to the TiAl alloy gave good result of modification of the cathodic process corresponding to a spontaneous passivation of the TiAl alloy. In solutions of high acidic concentration, the addition of PGMs shifted the cathodic process in the transpassive region, resulting in the dissolution of the alloy. The cathodic modification of PGM alloyed TiAl occurred as a result of PGM accumulation on the surface of the TiAl alloys, which simultaneously improved hydrogen evolution efficiency and inhibited anodic dissolution.

Acknowledgements

The authors would like to thank the Department of Science and Technology, Advanced Metals Initiative-Precious Metals Development Network and Mintek for permission to publish this work and financial support, and Wits for hosting the project. L.A. Cornish would like to thank the National Research Foundation.

References

1. H. A. Lipsitt: 'Titanium aluminides – an overview', *Mater. Res. Soc. Symp. Proc.*, 1984, **39**, 351–365.
2. J. H. Westbrook and R. L. Fleischer(eds): 'Intermetallic compounds, principles and practice', 2, Chap. 2, 91–131; 1995, Chichester, John Wiley & Sons Ltd.
3. J. H. Westbrook and R. L. Fleischer(eds): 'Intermetallic compounds, principles and practice', 2, Chap. 2, 73–90; 1995, Chichester, John Wiley & Sons Ltd.
4. J. H. Westbrook and R. L. Fleischer(eds): 'Intermetallic compounds, principles and practice', 2, Chap. 2, 147–173; 1995, Chichester, John Wiley & Sons Ltd.
5. S. Djanarthany, J.-C. Viala and J. Bouix: 'An overview of monolithic titanium aluminides based on Ti_3Al and TiAl', *Mater. Chem. Phys*., 2001, **72**, (3), 301–319.
6. O. Rivera-Denizard, N. Diffoot-Carlo, V. Navas and P. A. Sundaram: 'Biocompatibility studies of human foetal osteoblast cells cultured on gamma titanium aluminide', *J. Mater. Sci., Mater. Med.*, 2008, **19**, (1), 153–158.
7. B. B. Zhang, Y. F. Zheng and Y. Liu: 'Effect of Ag on the corrosion behaviour of Ti–Ag alloys in artificial saliva solutions', *Dent. Mater*., 2009, **25**, 672–677.
8. S. A. Bello, I. Maldonado, E. Rosim-Fachini, P. A. Sundaram and N. Diffoot-Carlo: 'In vitro evaluation of human osteoblast adhesion to a thermally oxidized γ-TiAl intermetallic alloy of composition Ti–48Al–2Cr–2Nb (at.%)', *J. Mater. Sci., Mater. Med.*, 2010, **21**, 1739–1750.
9. C. S. Brossia and G. A. Cragnolino: 'Effects of environmental and metallurgical conditions on the passive and localised dissolution of Ti–0·15%Pd', *Corrosion*, 2001, **9**, 768–779.
10. A. A. Trufanov, K. B. Katsov and M. V. Chervonyi: 'Effect of Ni and Mo additions on the corrosion-mechanical properties of Ti–Al alloy', *Khlorvinil Prod. Org. Kal.*, translated from *Fiziko-khimicheskaya Mekhanika Materialov*, 1989, **25**, (3), 28–32.
11. E. Van der Lingen and R. F. Sandenbergh: 'The cathodic modification behaviour of ruthenium additions to titanium in hydrochloric acid', *Corros. Sci*., 2001, **43**, 577–590.
12. R. F. Sandenbergh and E. van der Lingen: 'The use of Tafel back extrapolation to clarify the influence of ruthenium and palladium alloying on the corrosion behaviour of titanium in concentrated hydrochloric acid', *Corros. Sci*., 2005, **47**, 3300–3311.
13. R. W. Schutz: 'Ruthenium enhanced titanium alloys', *Platinum Met. Rev.*, 1996, **40**, (2), 54–61.
14. T. P. Hoar: 'Increasing the resistance of titanium to non-oxidising acids, influence of addition of platinum metals', *Platinum Met. Rev.*, 1960, **4**, (2), 59–64.
15. B. Cottis, M. Graham, R. Lindsay, S. Lyon, T. Richardson, D. Scandeburyand H. Scott(eds): 'Shreir's corrosion', 1st edn, 3, 'Corrosion and degradation of engineering materials', Chap. 3, 22, 'Corrosion of passive alloys: the effect of noble metal addition', 2224–2249; 2010, Amsterdam, Elsevier.
16. J. H. Potgieter and H. C. Brookes: 'Corrosion behaviour of a high-chromium duplex stainless steel with minor additions of ruthenium in sulfuric acid', *Corrosion*, 1995, **51**, (4), 312–320.
17. P. A. Olubambi, J. H. Potgieter and L. A. Cornish: 'Corrosion behaviour of superferritic stainless steels cathodically modified with minor additions of Ru in sulphuric and hydrochlorioc acid solutions', *Mater. Des*., 2009, **30**, (5), 1451–1457.
18. P. Monnartz: 'The study of the Fe–Cr alloys with particular regard to their solubility toward acids', *Metall*., 1911, 8, 161–176 and 193–209.
19. M. A. Streicher: 'Alloying stainless steel with the platinum metals increased resistance to corrosion in acids', *Platinum Met. Rev.*, 1977, **21**, (2), 51–55.
20. I. R. McGill: 'Platinum metals in stainless steels', *Platinum Met. Rev.*, 1990, **34**, (3), 144–154.
21. Y. H. Kim and G. S. Frankel: 'Effect of noble metal alloying on passivity and passivity breakdown of nickel', *J. Electrochem. Soc*., 2007,**154**, 36–42.
22. 'Standard practice for conventions applicable to electrochemical measurements in corrosion testing', G 3, 'Annual book of ASTM standards', ASTM, Philadelphia, PA, USA, 1985.
23. 'The titanium-aluminum (Ti-Al) phase diagram calculated with Thermo-Calc software, coupled with SSOL2 thermodynamic database'. http://www.calphad.com/pdf/Ti_Al_Phase_Diagram_Atomic_Pct_Celsius.pdf (accessed 22 Jun 2011).
24. A. Khataee, H. M. Flower and D. R. F. West: 'The alloying of titanium aluminides with ruthenium', *Platinum Met. Rev.*, 1989, **33**, (3), 106–113.
25. H. M. Saffarian, Q. Gan, R. Hadkar and G. W. Warren: 'Corrosion behaviour of binary titanium aluminide intermetallics', *Corros. Sci*., 1996, 626–633.
26. J. H. Potgieter, A. M. Heyns and W. Skinner: 'Cathodic modification as a mean of improving the corrosion resistance of alloys', *J. Appl. Electrochem.*, 1990, **20**, 711–715.

27. E. M. Sherif, JH. Potgieter, J. D. Comins, L. Cornish, P. A. Olubambi and C. N. Machio: 'Effects of minor additions of ruthenium on the passivation of duplex stainless-steel corrosion in concentrated hydrochloric acid solutions', *J. Appl. Electrochem.*, 2009, **39**, 1385–1392.
28. E. M. Sherif: 'Corrosion behaviour of duplex stainless steel alloy cathodically modified with minor ruthenium additions in concentrated sulfuric acid solutions', *Int. J. Electrochem. Sci.*, 2011, **6**, 2284–2298.
29. M. Pourbaix, N. de Zoubovand J. van Muylder(eds): 'Atlas d'équilibres électrochimiques', Chap. 4, 'Etablissement et interprétation de diagrammes d'équilibres tension-pH', 343–383 ; 1963, Paris, Publication du Centre Belge d'Etude de la Corrosion.